Saudi Pharmaceutical Journal 30 (2022) 369–376

Contents lists available at ScienceDirect

Saudi Pharmaceutical Journal

journal homepage: www.sciencedirect.com

Use of connectivity index and simple topological parameters for estimating the inhibition potency of acetylcholinesterase

Ante Miličević, Goran Šinko *

Institute for Medical Research and Occupational Health, Ksaverska cesta 2, HR-10 000 Zagreb, Croatia

ARTICLE INFO

Article history:
Received 8 November 2021
Accepted 30 January 2022
Available online 8 February 2022

Keywords:
Dementia
Alzheimer's disease
Inhibitor
Acetylcholinesterase
QSAR descriptor

ABSTRACT

Acetylcholinesterase (AChE) has proven to be an effective drug target in the treatment of neurodegenerative diseases such as Alzheimer's, Parkinson's and dementia. We developed a novel QSAR regression model for estimating potency to inhibit AChE, pK_i, on a set of 75 structurally different compounds including oximes, N-hydroxyiminoacetamides, 4-aminoquinolines and flavonoids. Although the model included only three simple descriptors, the valence molecular connectivity index of the zero-order, ${}^0\chi^v$, the number of 10-membered rings (nR10) and the number of hydroxyl groups (nOH), it yielded excellent statistics (r = 0.937, S.E. = 0.51). The stability of the model was evaluated when an initial set of 75 compounds was broadened to 165 compounds in total, with the increase of the range of pK_i (exp) from 6.0 to 10.2, yielding r = 0.882 and S.E. = 0.89. The predictive power of the model was evaluated by calculating pK_i values for 55 randomly chosen compounds ($S.E._{test}$ = 0.90) from the calibration model created on other 110 compounds (S.E. = 0.89), all taken from the pool of 165 compounds.
© 2022 The Author(s). Published by Elsevier B.V. on behalf of King Saud University. This is an open access article under the CC BY-NC-ND license (http://creativecommons.org/licenses/by-nc-nd/4.0/).

1. Introduction

Acetylcholinesterase (AChE) have proven to be effective in the treatment of Alzheimer's and Parkinson's disease symptoms. The current treatment is based on AChE inhibitors including donepezil, rivastigmine and alkaloid galantamine (Giacobini, 2006; Mohammad et al., 2017; Xie et al., 2020). Although Tacrine (Cognexw®) was approved as a drug for AD treatment, it was discontinued from medical use due to high hepatotoxicity. Therefore, with the ageing of the world population and increased risk of dementia, the development of AChE inhibitors attracts the highest scientific interest in the process of designing safer and more effective drugs (Sanad and Mekky, 2021; Xie et al., 2020).

The QSAR (quantitative structure–activity relationship) method represents an important tool for drug development and has led to numerous AChE QSAR models (Jana et al., 2018; Kumar et al., 2020; Niu et al., 2017) of different complexity and predictivity. The development of a QSAR regression model could facilitate the development of therapeutic ligands by establishing a correlation between the chemical functionalities of the ligand and the desired biological activity. The proposed regression model comprised of the molecular parameters (descriptors) of interest would enable the prediction of biological activity and ease the design of new compounds with the desired activity (Kubinyi, 1993; Karelson, 2000; Selassie and Verma, 2010). The activity prediction of a QSAR model and its accuracy is based on the selection of appropriate molecular descriptors and the reliability of the measured biological activity (Leach, 1996; Shityakov et al., 2014).

The potential of QSAR models using scoring functions to predict the inhibition potency of acetylcholinesterase (AChE) ligands was analyzed in a recent study (Šinko, 2019). The study indicated that the PLP2 scoring function predicts the inhibition potency of ligands with a coefficient of determination r^2 = 0.591. Several scoring functions were tested against AChE-ligand complexes deposited in the PDB base: LigScore1, LigScore2, PLP1, PLP2, Jain, PMF and PMF04. The study showed that the drawback of the scoring function evaluation was the low uniformity of kinetic data (K_i or IC_{50}) obtained using various methods of determination and the enzyme source. Kinetic data were collected under different experimental conditions, i.e. temperature, as well as using various enzyme species as a source of AChE, one species for data measurements and another for the determination of the crystal structure of the AChE-ligand complex.

* Corresponding author.
E-mail address: gsinko@imi.hr (G. Šinko).
Peer review under responsibility of King Saud University.

Production and hosting by Elsevier

https://doi.org/10.1016/j.jsps.2022.01.025
1319-0164/© 2022 The Author(s). Published by Elsevier B.V. on behalf of King Saud University.
This is an open access article under the CC BY-NC-ND license (http://creativecommons.org/licenses/by-nc-nd/4.0/).

It was interesting to see that studies using the same ligand, e.g. galantamine, and AChE from the same source *Electrophorus electricus* may differ in the obtained results due to measuring the IC_{50} (0.36–1.07 μM) (Atanasova et al., 2015; Mary et al., 1998) instead of the K_i (0.19 μM) (Rahman et al., 2006). Uncertainty in the IC_{50} value determination is caused by the type and concentration of the substrate used for measurements and therefore K_i is a more reliable parameter, as it is a measure of enzyme ligand affinity in the absence of a substrate. The negative effect of the solvent mixture on the AChE enzyme activity when using ethanol or DMSO buffer should be tested, as ethanol or DMSO apparently increase the ligand inhibition potency due to AChE inhibition (Fekonja et al., 2007; Kumar and Darreh-Shori, 2017). Therefore, the effect of a solvent on AChE activity needs to be characterized and compensated properly.

In a study by Wong et al., the problem of various enzyme sources in a QSAR analysis of tacrine-like inhibitors was reported. Therefore, they created 10 different QSAR regression models for each AChE source, e.g. human, *Electrophorus electricus* and bovine AChE (Wong et al., 2014). The inhibition potency of tacrine-like inhibitors was evaluated by the Ellman (Ellman et al., 1961) or Rappaport method (Rappaport et al., 1959) using acetylthiocholine iodide or acetylcholine chloride, respectively, as the substrate. The reported IC_{50} values, obtained using different experimental conditions, led to the development of different QSAR regression models to increase model predictivity and overcome the problem of experimental conditions.

The goal of this study was to highlight the key structural features of AChE ligands in correlation with ligand pK_i values indicating inhibitory activity using the simplest possible QSAR model. The different QSAR models presented in the literature describe various parameters for AChE ligands, but often these parameters cannot be easily linked to a ligand's physicochemical properties (Gurung et al., 2017; Jana et al., 2018; Šinko, 2019; Wong et al., 2014). In our approach, we developed a simple QSAR model for the prediction of the human AChE inhibition constant, pK_i, on a set of 75 compounds including 4-aminoquinolines, oximes, flavonoids and *N*-hydroxyiminoacetamides. For all of the compounds in this study, K_i was measured by our laboratory and published previously (Tables 1 and S3, Fig. 1) (Bosak et al., 2019, 2017; Bušić et al., 2016; Katalinić et al., 2010; Kovarik et al., 2008; Maček Hrvat et al., 2020; Maraković et al., 2020, 2016; Šinko et al., 2010; Zandona et al., 2020). The assay used for the AChE activity measurement was based on the Ellman method (Ellman et al., 1961), with standardized activity measurement regarding enzyme, substrate and inhibitor concentrations (Eyer et al., 2003; Reiner et al., 2000). To avoid the artefacts of K_i calculation, AChE inhibition was limited for 20–80% of the control activity (Bosak et al., 2019; Simeon-Rudolf et al., 2001). Moreover, AChE activities were corrected when the oxime-induced degradation of the substrate (oximolysis) was above 10% of the enzyme control activity (Maček Hrvat et al., 2018; Šinko et al., 2007, 2006).

2. Materials and methods

2.1. Calculation of topological indices

Molecular descriptors were calculated by the E-DRAGON program developed by Tetko et al. E-DRAGON provides more than 1 600 molecular descriptors (topological, constitutional, geometrical, etc.) in a single run (Tetko et al., 2005). The connectivity matrices were constructed using the *Online SMILES Translator and Structure File Generator* (Online SMILES Translator and Structure File Generator, 2020). The SMILE formulas, for all compounds studied, are given in Supplement (Tables S3, S4 and S5).

The model developed in this study is based on the topological ${}^0\chi^v$ index (the valence molecular connectivity index of the zero-order) (Kier and Hall, 1986, 1976a, 1976b; Randić, 2008), which was defined as:

$$ {}^0\chi^v = \sum_i \delta(i)^{-0.5} \tag{1}$$

where $\delta(i)$ is the weight (valence value) of each vertex (atom) i in a vertex-weighted molecular graph. The valence value, $\delta(i)$, of vertex i is defined as:

$$ \delta(i) = [Z^v(i) - H(i)]/[Z(i) - Z^v(i) - 1] \tag{2}$$

where $Z^v(i)$ is the number of valence electrons belonging to the atom corresponding to vertex i, $Z(i)$ is its atomic number, and $H(i)$ is the number of hydrogen atoms attached to it. For instance, the delta values for the primary, secondary, tertiary, and quaternary carbon atoms are 1, 2, 3, and 4, respectively, while for the oxygen in the OH group, this equals 5 and for the NH_2 group 3. It should be pointed out that ${}^0\chi^v$ is the only one of the many members from the family of valence connectivity indices ${}^n\chi^v$, which differ amongst each other by path length, i.e. the number of consecutive chemical bonds. From Eq. (1) it can be seen that ${}^0\chi^v$ has a path order of zero, i.e. it considers only separate vertices (atoms). ${}^1\chi^v$ ($ {}^1\chi^v = \Sigma\ [\delta(i)\ \delta(j)]^{-0.5}$) considers vertices (atoms) i and j, making up a path with a length of 1 (one consecutive chemical bond), ${}^2\chi^v$ ($ {}^2\chi^v = \Sigma\ [\delta(i)\ \delta(j)\ \delta(k)]^{-0.5}$) considers vertices (atoms) i, j and k, making up a path with a length of 2 (two consecutive chemical bonds), etc. Connectivity indices are also called branching indices and are among the most used topological indices in QSPR/QSAR, e.g. ${}^3\chi^v$ was very successfully used for the estimation of the stability constants of metal chelates (Miličević and Raos, 2008; Raos et al., 2008).

2.2. Regression calculations

Regression calculations, including the leave-one-out procedure (LOO) of cross validation, were done using the CROMRsel program (Lučić and Trinajstić, 1999). The standard error of the cross-validation estimate was defined as:

$$ S.E_{cv} = \sqrt{\sum_i \frac{\Delta X_i^2}{N}} \tag{3}$$

where ΔX and N denote cv residuals and the number of reference points, respectively.

3. Results and discussion

Although the correlation of the valence molecular connectivity index of the zero-order, ${}^0\chi^v$, on pK_i, yields somewhat worse statistics (r = 0.795 and S.E. = 0.88, N = 75) than the correlation with the squared Ghose-Crippen octanol–water partition coefficient, AlogP2, (r = 0.857 and S.E. = 0.74, N = 75) and a few other topological indices, it has captured our attention. More precisely, considering the presence of a 10-membered ring (two fused six-membered rings) in the molecule, two almost parallel correlation lines on ${}^0\chi^v$ *vs.* pK_i dependence can be drawn (Fig. 2). The first line (triangles in Fig. 2, r = 0.800, N = 26) belongs to molecules with a 10-membered ring and the second (circles in Fig. 2, r = 0.575, N = 49) is without a 10-membered ring. It can also be seen that molecules with a 10-membered ring in their structure generally have higher values of pK_i. Flavonoids (**27**–**34**) are the only compounds for which this does not apply, but their structure is highly rigid in comparison with other compounds with a 10-membered ring. This is especially true for the flavonoid rutin (**34**), which by far has the highest number of OH groups (10 hydroxyl groups) of all molecules in the set.

Table 1
The values of negative logarithms of the AChE inhibition constant (pK_i), and molecular descriptors for 75 compounds. $^0\chi^v$, nOH and nR10 were calculated by the E-DRAGON program system. The compound names are the same as in the original papers whose references are given.

No.	Compound	pK_i	$^0\chi^v$	nOH	nR10
1	ICD-585[a]	4.55	11.70	1	0
2	HI-6[a]	4.51	11.40	1	0
3	HLo-7[a]	4.62	12.79	2	0
4	K027[a]	4.14	11.70	1	0
5	K048[a]	3.96	12.41	1	0
6	K033[a]	4.77	12.39	2	0
7	TMB-4[a]	3.74	11.68	2	0
8	DMB-4[a]	4.00	10.98	2	0
9	MMB-4[a]	3.31	10.27	2	0
10	ICD-692[a]	4.74	11.99	1	0
11	ICD-467[a]	5.92	11.53	1	0
12	K114[b]	5.68	14.29	2	0
13	K127[b]	3.76	12.81	1	0
14	K203[b]	4.44	12.15	1	0
15	I[c]	2.93	9.610	1	0
16	II[c]	3.45	14.08	1	0
17	III[c]	4.31	14.93	1	0
18	IV[c]	3.87	15.41	2	0
19	CQ[d]	4.96	7.050	0	1
20	CQ2[d]	5.39	8.96	0	1
21	TFCQ2[d]	5.44	9.46	0	1
22	TFCQ8[d]	6.34	13.70	0	1
23	CQ8[d]	6.21	13.20	0	1
24	CQAd[d]	6.11	16.77	0	1
25	Chloroquine[d]	5.40	14.53	0	1
26	CQEtOH[d]	5.00	8.83	1	1
27	Galangin[e]	4.07	10.20	3	1
28	Kaempferol[e]	4.03	10.57	4	1
29	Quercitin[e]	4.42	10.94	5	1
30	Myricetin[e]	4.42	11.31	6	1
31	Luteolin[e]	4.18	10.57	4	1
32	Fisetin[e]	4.00	10.57	4	1
33	Apigenin[e]	3.92	10.20	3	1
34	Rutin[e]	3.52	22.29	10	1
35	Metaproterenol[f]	2.51	8.94	3	0
36	Terbutaline[f]	2.32	9.86	3	0
37	Fenoterol[f]	3.07	12.40	4	0
38	Epinephrine[f]	2.19	7.36	3	0
39	Isoproterenol[f]	2.60	8.94	3	0
40	Isoetharine[f]	3.68	10.51	3	0
41	Salbutamol[f]	2.70	10.57	3	0
42	Salmeterol[f]	4.52	17.93	3	0
43	1[g]	3.64	12.15	3	0
44	2[g]	3.36	12.45	3	0
45	3[g]	3.90	13.21	3	0
46	4[g]	4.12	14.04	3	0
47	5[g]	3.78	13.34	3	0
48	6[g]	3.98	13.08	3	0
49	7[g]	4.05	13.48	3	0
50	8[g]	3.90	13.48	3	0
51	9[g]	3.90	15.46	3	0
52	1a[h]	7.82	23.95	1	1
53	2a[h]	8.22	24.65	1	1
54	1b[h]	8.05	24.65	1	1
55	2b[h]	7.55	25.36	1	1
56	1c[h]	7.17	25.36	1	1
57	2c[h]	7.49	26.07	1	1
58	1d[h]	6.89	23.95	1	1
59	2d[h]	7.64	24.65	1	1
60	1e[h]	7.39	24.65	1	1
61	2e[h]	7.00	25.36	1	1
62	Q1[i]	2.42	5.96	1	0
63	Q2[i]	3.12	7.01	1	0
64	Q3[i]	3.28	8.00	1	0
65	Q4[i]	3.26	8.71	1	0
66	Q5[i]	5.22	14.79	1	0
67	Q6[i]	3.80	10.1	1	0

(*continued on next page*)

Table 1 (*continued*)

No.	Compound	pK_i	$^0\chi^v$	nOH	nR10
68	Q7[i]	4.49	11.99	1	0
69	Q8[i]	4.17	11.99	1	0
70	Q9[i]	4.39	11.16	1	0
71	Q10[i]	4.04	11.16	1	0
72	Q11[i]	4.57	11.02	1	0
73	Q12[i]	3.87	11.02	1	0
74	Q13[i]	4.74	11.29	1	0
75	Q14[i]	4.31	11.29	1	0

[a] From Ref. (Kovarik et al., 2008).
[b] From Ref. (Šinko et al., 2010).
[c] From Ref. (Maraković et al., 2016).
[d] From Ref. (Bosak et al., 2019).
[e] From Ref. (Katalinić et al., 2010).
[f] From Ref. (Bosak et al., 2017).
[g] From Ref. (Bušić et al., 2016).
[h] From Ref. (Maček Hrvat et al., 2020).
[i] From Ref. (Zandona et al., 2020).

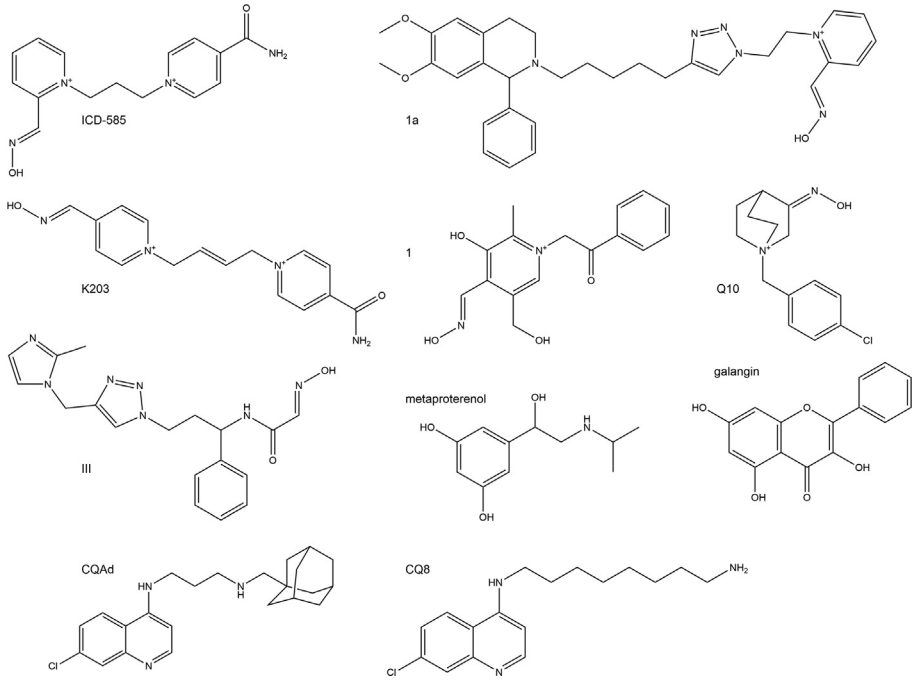

Fig. 1. Example of chemical structures of the 10 groups of compounds used in the set of 75 compounds.

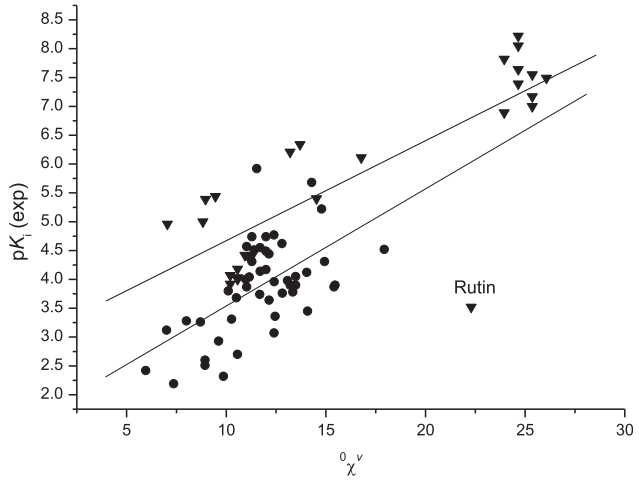

Fig. 2. Dependence of pK_i on the $^0\chi^v$ index for 75 molecules in the set (Table 1). The lines of correlations are made on two subsets of molecules, with (N = 26, r = 0.800) and without (N = 49, r = 0.575) a 10-membered ring. Triangles denote molecules with a 10-membered ring.

All these were the reason why we added nR10 and nOH descriptors alongside $^0\chi^v$ into the equation. In that way, we developed three descriptor model for the estimation of pK_i:

$$pK_i = a + b_1 \cdot {}^0\chi^v + b_2 \cdot \mathrm{nR10} + b_3 \cdot \mathrm{nOH} \quad (4)$$

yielding r = 0.937, S.E. = 0.51 and S.E.$_{cv}$ = 0.53 (a = 2.54(19), b_1 = 0.170(13), b_2 = 1.13(14), b_3 = –0.353(38)) for the set of 75 compounds, Fig. 3. It is also important to note that the correlations between the pairs of descriptors were very small; r = 0.233, 0.123 and 0.483 for nOH *vs.* nR10, $^0\chi^v$ *vs.* nOH and $^0\chi^v$ *vs.* nR10, respectively.

Some topological and constitutional descriptors correlated to pK_i showed similar statistics and a similar pattern as $^0\chi^v$, like the valence molecular connectivity index of the first order, $^1\chi^v$, the eccentric connectivity index, CSI, and the number of atoms, nAT (r = 0.809, 0.798 and 0.777, respectively). Their implementation in Eq. (4) in place of $^0\chi^v$ yielded slightly worse statistics (S.E. = 0.53, 0.55 and 0.54, respectively) than the standard error obtained by $^0\chi^v$ (S.E. = 0.51).

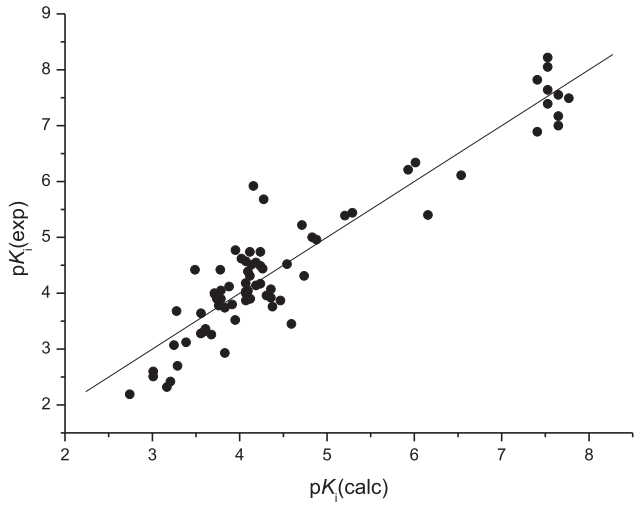

Fig. 3. Plot of experimental *vs.* calculated (using Eq. (4)) pK_i values; N = 75, r = 0.937, S.E. = 0.51 and S.E.$_{cv}$ = 0.53.

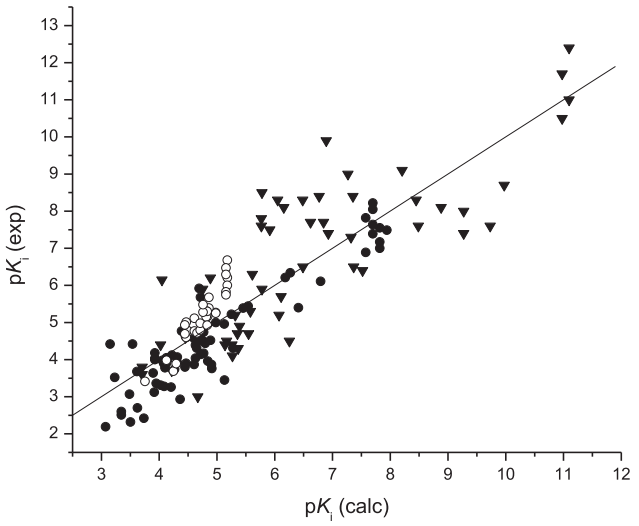

Fig. 4. Plot of experimental *vs.* calculated (using Eq. (4)) pK_i (or pIC_{50}) values; N = 165, r = 0.882, r_{cv} = 0.874, S.E. = 0.89 and S.E.$_{cv}$ = 0.91. Circles denote the set of 75 compounds, triangles the set of 56 compounds used in our previous report (Šinko, 2019), and empty circles the set of 34 oximes (Katalinić et al., 2016).

Although the best possible model with three descriptors chosen among all of the 1399 calculated descriptors gave better results than Eq. (4) (r = 0.952, S.E. = 0.44 and S.E.$_{cv}$ = 0.47), the descriptors used in that model were not easy to connect to the structure of compounds; highest eigenvalue number of Burden matrix weighted by atomic Sanderson electronegativities (BEHe1), 3D-MoRSE - signal 13 weighted by atomic van der Waals volumes (Mor13v) and the difference between multiple path count and path count (PCD).

Previously (Šinko, 2019) we evaluated models using scoring functions for the pK_i (or pIC_{50}) estimation of 56 molecules (Tables S1 and S4). By applying our model (Eq. (4)) on the same set of compounds, the statistics were not so good, r = 0.830, r_{cv} = 0.798, S.E. = 1.20 and S.E.$_{cv}$ = 1.30, but one must be aware that the K_i (AChE) values for this set were not measured by the same laboratory and on the same type of AChE (they used human, mouse, *etc.*). Moreover, instead of K_i, for some molecules IC_{50} values (Rahman et al., 2006; Atanasova et al., 2015; Herkert et al., 2011; Mary et al., 1998; Saxena et al., 1999) were given. However, when we brought together this set of 56 compounds with our set of 75 compounds, the results of regression on 131 molecules were very good (N = 131, r = 0.892, r_{cv} = 0.883, S.E. = 0.94 and S.E.$_{cv}$ = 0.97), especially as the range of experimental pK_i (or pIC_{50}) increased from 6.03 to 10.21.

We also used 34 oximes, Tables S2 and S5, from our previous paper (Katalinić et al., 2016), where we showed that pIC_{50} can be estimated by using only one topological index; the model using eccentric connectivity index (CSI, Sharma et al., 1997) yielded r = 0.957, S.E. = 0.21 and S.E.$_{cv}$ = 0.23. The $^0\chi^v$ index yielded slightly worse but also excellent results (r = 0.926, S.E. = 0.27 and S.E.$_{cv}$ = 0.29). Combining this set of 34 compounds with two sets presented above (N = 75 and N = 56), our model (Eq. (4)) yielded r = 0.882, S.E. = 0.89 and S.E.$_{cv}$ = 0.91 (a = 3.17(23), b_1 = 0.172 (17), b_2 = 0.753(90), b_3 = –0.451(55); N = 165, Fig. 4). Comparing these regression parameters (on a set of 165 molecules) with the parameters in the model for the 75-member set (a = 2.54(19), b_1 = 0.170(13), b_2 = 1.13(14), b_3 = –0.353(38)) great similarity can be observed, although within the limits of S.E. only for $^0\chi^v$ (b_1 = 0.172(16) *vs.* 0.170(13)).

We tested the predictability of our model (Eq. (4)) by a training/test method. We selected every third molecule (molecules **3, 6, 9, 12**..., Table 1, S1 and S2) into the test set and thereby divided the set of 165 compounds into a training set (110 compounds) and test set (55 compounds). Statistics of the calibration model calculated from Eq. (4) on the training set (r = 0.882, S.E. = 0.89 and S.E.$_{cv}$ = 0.92, N = 110) were of the same quality as the model made on 165 compounds and we used it for predicting the pK_i values of 55 molecules from the test set. The standard error of the test set (S.E.$_{test}$ = 0.90) was very similar to the S.E. and S.E.$_{cv}$ of the calibration model (S.E. = 0.89 and S.E.$_{cv}$ = 0.92), which proved the high predictive power of Eq. (4).

A comparison of the AChE active site amino acid composition and related functional characteristics with the QSAR descriptors $^0\chi^v$, nR10 and nOH led us to the following observations. The human AChE active site gorge is a ~20 Å deep and ~5 Å wide cavity composed of mainly aromatic residues (Phe, Trp or Tyr) thus creating a hydrophobic space (Ordentlich et al., 1993; Sussman et al., 1991). At the bottom of the narrow active site, where substrate hydrolysis occurs, a catalytic triad Ser203, Glu334 and His447 is located (Fig. 5). The substrate of AChE is a small carboxyl ester with a positively charged choline part, acetylcholine. During acetylcholine hydrolysis, the following key interactions between enzyme residues and substrate formed: hydrogen bonds, hydrophobic interactions and cation-π interactions (Colletier et al., 2006). Ligands that can create these interactions producing strong binding within the AChE active site are possible drug candidates.

Several residues of the AChE active site: Asp74, Glu202, Tyr124, Ser293 and Tyr337 have hydrogen bond donor or acceptor groups, and therefore may stabilize ligands *via* hydrogen bonds (Šinko, 2019). Hydrogen bond donors or acceptor groups are the molecular basis for an nOH descriptor presence in the QSAR model. Two important sub-domains of the AChE catalytic site, the peripheral anionic site and choline binding site, are responsible for substrate transport and orientation during catalytic turnover (Colletier et al., 2006). Tryptophan Trp86 and Trp286 are key residues of the choline binding site and peripheral anionic site, respectively (Colletier et al., 2006; Ordentlich et al., 1993). These two residues create cation-π and/or π-π interactions with ligands having aromatic groups; e.g. two fused benzene rings (nR10) in quinolines or benzopyrans create π-π stabilizing interactions by overlapping with Trp indole ring. Studies have shown that ligands long enough to bind simultaneously in the choline binding site and the peripheral anionic site are more potent inhibitors of AChE, e.g. donepezil depicted in Fig. 5 (Bourne et al., 2016; Cheung et al., 2012; Felder

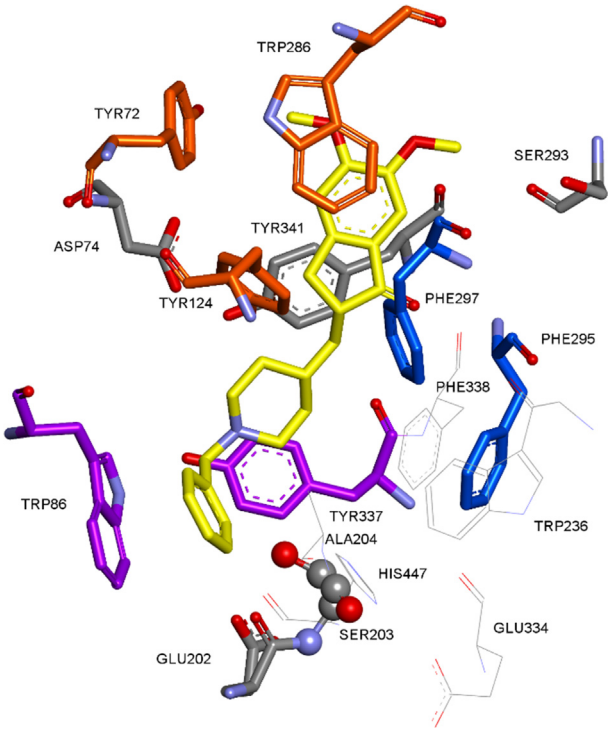

Fig. 5. Crystal structure of the human AChE active site (PDB ID 4EY7). Aromatic residues of the peripheral anionic site are orange, of the choline binding site purple, and of the acyl pocket blue. The anti-Alzheimer drug donepezil is yellow. Catalytic Ser203 is represented by a ball and stick. Figure adopted from ref. (Miličević and Šinko, 2021).

et al., 2002; Rydberg et al., 2006). Crystal structures of AChE-ligand complexes showed that the binding would be stronger if the conformation of the residues stabilizing the ligand was complementary to the conformation of the apo-AChE active site, e.g. donepezil only affects the conformation of Tyr337, while conformation of the other residues remained unchanged (Cheung et al., 2012; Gerlits et al., 2019). It has been shown that some ligands upon binding induce the change of the conformation of the AChE active site residues (Bourne et al., 2010), therefore there is no clear connection between active site residues conformation and the strength of ligand binding (Šinko, 2019). Index ${}^{0}\chi^{v}$ accounts for the size of the ligand but more importantly for the complexity of the ligand structure, including branching. We showed a positive correlation between ${}^{0}\chi^{v}$ and pK_i in Fig. 2. A similar finding was presented in a prior study where the complexity property of ligands positively correlated with the scoring functions was described (Šinko, 2019).

4. Conclusions

The presented QSAR model (Eq. (4)) is based on the valence molecular connectivity index of the zero-order, ${}^{0}\chi^{v}$, combined with the number of 10-membered rings (nR10) and the total number of OH groups in a molecule (nOH). On a set of 75 molecules, the model yielded S.E. = 0.51, meaning that pK_i (or pIC_{50}) values can be estimated by an error of 8.5% of the pK_i range ((S.E./range pK_i) 100%). Although the model on 131 compounds, after adding 56 compounds from the literature (Rahman et al., 2006; Atanasova et al., 2015; Herkert et al., 2011; Mary et al., 1998; Saxena et al., 1999) seemed to deteriorate (S.E. = 0.94), ultimately this was not the case. The reason was that the pK_i (or pIC_{50}) range increased from 6.03 to 10.21, so, although the S.E. almost doubled, the error of estimation increased only slightly, to 9.2%. This, and especially the regression on 56 molecules (S.E. = 1.20, with an error of estimation of 12.8%), told us that QSAR should be avoided on non-standardized experimental data. When we added 34 oximes (IC_{50} measured in our laboratory) to the set of 131 compounds, the range of pK_i (or pIC_{50}) values stayed the same, and the S.E. and error of estimation dropped to 0.89 and 8.7%, respectively.

Comparing errors of estimation yielded by Eq. (4) with the mean experimental error in K_i measurements, which was 15% for the set of 75 molecules, we can conclude that our results are very satisfactory (Raos et al., 2008; Raos and Miličević, 2016). This is proof that the variables we used in our three-descriptor model (${}^{0}\chi^{v}$, nR10 and nOH) were profoundly chosen according to the structural features of the compounds and AChE active site. Furthermore, unlike some of the molecular descriptors usually used in QSAR models (Gurung et al., 2017; Wong et al., 2014), our variables are simple and easy to explain.

CRediT authorship contribution statement

Ante Miličević: Conceptualization, Methodology, Data curation, Writing – original draft, Writing – review & editing. **Goran Šinko:** Conceptualization, Data curation, Writing – original draft, Writing – review & editing.

Declaration of Competing Interest

The authors declare that they have no known competing financial interests or personal relationships that could have appeared to influence the work reported in this paper.

Acknowledgement

This study is a modified version of the previously published and retracted study Miličević and Šinko, Eur J Pharm Sci 160 (2021) 105757 (without entries 76–94 in Table 1).

Funding

This study was funded by the Croatian Ministry of Science and Education.

Appendix A. Supplementary material

Supplementary data to this article can be found online at https://doi.org/10.1016/j.jsps.2022.01.025.

References

Atanasova, M., Stavrakov, G., Philipova, I., Zheleva, D., Yordanov, N., Doytchinova, I., 2015. Galantamine derivatives with indole moiety: docking, design, synthesis and acetylcholinesterase inhibitory activity. Bioorg. Med. Chem. 23 (17), 5382–5389. https://doi.org/10.1016/j.bmc.2015.07.058.

Bosak, A., Knežević, A., Gazić Smilović, I., Šinko, G., Kovarik, Z., 2017. Resorcinol-, catechol- and saligenin-based bronchodilating β2-agonists as inhibitors of human cholinesterase activity. J. Enzyme Inhib. Med. Chem. 32 (1), 789–797. https://doi.org/10.1080/14756366.2017.1326109.

Bosak, A., Opsenica, D.M., Šinko, G., Zlatar, M., Kovarik, Z., 2019. Structural aspects of 4-aminoquinolines as reversible inhibitors of human acetylcholinesterase and butyrylcholinesterase. Chem. Biol. Interact. 308, 101–109. https://doi.org/10.1016/j.cbi.2019.05.024.

Bourne, Y., Radić, Z., Taylor, P., Marchot, P., 2010. Conformational remodeling of femtomolar inhibitor–acetylcholinesterase complexes in the crystalline state. J. Am. Chem. Soc. 132 (51), 18292–18300. https://doi.org/10.1021/ja106820e.

Bourne, Y., Sharpless, K.B., Taylor, P., Marchot, P., 2016. Steric and dynamic parameters influencing in situ cycloadditions to form triazole inhibitors with crystalline acetylcholinesterase. J. Am. Chem. Soc. 138 (5), 1611–1621. https://doi.org/10.1021/jacs.5b11384.

Bušić, V., Katalinić, M., Šinko, G., Kovarik, Z., Gašo-Sokač, D., 2016. Pyridoxal oxime derivative potency to reactivate cholinesterases inhibited by organophosphorus

compounds. Toxicol. Lett. 262, 114–122. https://doi.org/10.1016/j.toxlet.2016.09.015.
Cheung, J., Rudolph, M.J., Burshteyn, F., Cassidy, M.S., Gary, E.N., Love, J., Franklin, M. C., Height, J.J., 2012. Structures of human acetylcholinesterase in complex with pharmacologically important ligands. J. Med. Chem. 55 (22), 10282–10286. https://doi.org/10.1021/jm300871x.
Colletier, J.-P., Fournier, D., Greenblatt, H.M., Stojan, J., Sussman, J.L., Zaccai, G., Silman, I., Weik, M., 2006. Structural insights into substrate traffic and inhibition in acetylcholinesterase. EMBO J. 25 (12), 2746–2756. https://doi.org/10.1038/sj.emboj.7601175.
Ellman, G.L., Courtney, K.D., Andres, V., Featherstone, R.M., 1961. A new and rapid colorimetric determination of acetylcholinesterase activity. Biochem. Pharmacol. 7 (2), 88–95. https://doi.org/10.1016/0006-2952(61)90145-9.
Eyer, P., Worek, F., Kiderlen, D., Sinko, G., Stuglin, A., Simeon-Rudolf, V., Reiner, E., 2003. Molar absorption coefficients for the reduced Ellman reagent: reassessment. Anal. Biochem. 312 (2), 224–227. https://doi.org/10.1016/S0003-2697(02)00506-7.
Fekonja, O., Zorec-Karlovšek, M., Kharbili, M.E., Fournier, D., Stojan, J., 2007. Inhibition and protection of cholinesterases by methanol and ethanol. J. Enzyme Inhib. Med. Chem. 22 (4), 407–415. https://doi.org/10.1080/14756360601143857.
Felder, C.E., Harel, M., Silman, I., Sussman, J.L., 2002. Structure of a complex of the potent and specific inhibitor BW284C51 with Torpedo californica acetylcholinesterase. Acta Crystallogr. Sect. D Biol. Crystallogr. 58 (10), 1765–1771. https://doi.org/10.1107/S0907444902011642.
Gerlits, O., Ho, K.-Y., Cheng, X., Blumenthal, D., Taylor, P., Kovalevsky, A., Radić, Z., 2019. A new crystal form of human acetylcholinesterase for exploratory room-temperature crystallography studies. Chem. Biol. Interact. 309, 108698. https://doi.org/10.1016/j.cbi.2019.06.011.
Giacobini, E., 2006. Cholinesterases in human brain: the effect of cholinesterase inhibitors on Alzheimer's disease and related disorders. In: Giacobini, E., Pepeu, G. (Eds.), The Brain Cholinergic System. CRC Press, pp. 235–264. https://doi.org/10.1201/b14486-19.
Gurung, A.B., Aguan, K., Mitra, S., Bhattacharjee, A., 2017. Identification of molecular descriptors for design of novel Isoalloxazine derivatives as potential Acetylcholinesterase inhibitors against Alzheimer's disease. J. Biomol. Struct. Dyn. 35 (8), 1729–1742. https://doi.org/10.1080/07391102.2016.1192485.
Herkert, N.M., Thiermann, H., Worek, F., 2011. In vitro kinetic interactions of pyridostigmine, physostigmine and soman with erythrocyte and muscle acetylcholinesterase from different species. Toxicol. Lett. 206 (1), 41–46. https://doi.org/10.1016/j.toxlet.2011.03.004.
Jana, S., Ganeshpurkar, A., Singh, S.K., 2018. Multiple 3D-QSAR modeling, e-pharmacophore, molecular docking, and in vitro study to explore novel AChE inhibitors. RSC Adv. 8 (69), 39477–39495. https://doi.org/10.1039/C8RA08198K.
Mati Karelson, 2000. No TitleMolecular Descriptors in QSAR/QSPR, 1st editio. ed. Wiley-Interscience, New York. <https://doi.org/9>.
Katalinić, M., Rusak, G., Domaćinović Barović, J., Šinko, G., Jelić, D., Antolović, R., Kovarik, Z., 2010. Structural aspects of flavonoids as inhibitors of human butyrylcholinesterase. Eur. J. Med. Chem. 45 (1), 186–192. https://doi.org/10.1016/j.ejmech.2009.09.041.
Katalinić, M., Maček Hrvat, N., Baumann, K., Morasi Piperčić, S., Makarić, S., Tomić, S., Jović, O., Hrenar, T., Miličević, A., Jelić, D., Žunec, S., Primožič, I., Kovarik, Z., 2016. A comprehensive evaluation of novel oximes in creation of butyrylcholinesterase-based nerve agent bioscavengers. Toxicol. Appl. Pharmacol. 310, 195–204. https://doi.org/10.1016/j.taap.2016.09.015.
Kier, L.B., Hall, L.H., 1976a. Molecular Connectivity in Chemistry and Drug Research. Academic Press, New York.
Kier, L.B., Hall, L.H., 1976b. Molecular connectivity vii: specific treatment of heteroatoms. J. Pharm. Sci. 65 (12), 1806–1809. https://doi.org/10.1002/jps.2600651228.
Kier, L.B., Hall, L.H., 1986. Molecular Connectivity in Structure-Activity Analysis. Willey, New York.
Kovarik, Z., Čalić, M., Bosak, A., Šinko, G., Jelić, D., 2008. In vitro evaluation of aldoxime interactions with human acetylcholinesterase. Croat. Chem. Acta 81, 47–57 https://hrcak.srce.hr/file/36860.
Kubinyi, H., 1993. QSAR: Hansch Analysis and Related Approaches, Methods and Principles in Medicinal Chemistry. Wiley, Weinheirn. <https://doi.org/10.1002/9783527616824>.
Kumar, A., Darreh-Shori, T., 2017. DMSO: a mixed-competitive inhibitor of human acetylcholinesterase. ACS Chem. Neurosci. 8 (12), 2618–2625. https://doi.org/10.1021/acschemneuro.7b00344.
Kumar, V., Saha, A., Roy, K., 2020. In silico modeling for dual inhibition of acetylcholinesterase (AChE) and butyrylcholinesterase (BuChE) enzymes in Alzheimer's disease. Comput. Biol. Chem. 88, 107355. https://doi.org/10.1016/j.compbiolchem.2020.107355.
Leach, A.R., 1996. Molecular Modelling: Principles and Applications. Longman.
Lučić, B., Trinajstić, N., 1999. Multivariate regression outperforms several robust architectures of neural networks in QSAR modeling. J. Chem. Inf. Comput. Sci. 39 (1), 121–132. https://doi.org/10.1021/ci980090f.
Maček Hrvat, N., Zorbaz, T., Šinko, G., Kovarik, Z., 2018. The estimation of oxime efficiency is affected by the experimental design of phosphylated acetylcholinesterase reactivation. Toxicol. Lett. 293, 222–228. https://doi.org/10.1016/j.toxlet.2017.11.022.
Maček Hrvat, N., Kalisiak, J., Šinko, G., Radić, Z., Sharpless, K.B., Taylor, P., Kovarik, Z., 2020. Evaluation of high-affinity phenyltetrahydroisoquinoline aldoximes, linked through anti-triazoles, as reactivators of phosphylated cholinesterases. Toxicol. Lett. 321, 83–89. https://doi.org/10.1016/j.toxlet.2019.12.016.
Maraković, N., Knežević, A., Vinković, V., Kovarik, Z., Šinko, G., 2016. Design and synthesis of N-substituted-2-hydroxyiminoacetamides and interactions with cholinesterases. Chem. Biol. Interact. 259, 122–132. https://doi.org/10.1016/j.cbi.2016.05.035.
Maraković, N., Knežević, A., Rončević, I., Brazzolotto, X., Kovarik, Z., Šinko, G., 2020. Enantioseparation, in vitro testing, and structural characterization of triple-binding reactivators of organophosphate-inhibited cholinesterases. Biochem. J. 477, 2771–2790. https://doi.org/10.1042/BCJ20200192.
Mary, A., Renko, D.Z., Guillou, C., Thal, C., 1998. Potent acetylcholinesterase inhibitors: design, synthesis, and structure–activity relationships of bis-interacting ligands in the galanthamine series. Bioorg. Med. Chem. 6 (10), 1835–1850. https://doi.org/10.1016/S0968-0896(98)00133-3.
Miličević, A., Raos, N., 2008. Influence of chelate ring interactions on copper(II) chelate stability studied by connectivity index functions. J. Phys. Chem. A 112 (33), 7745–7749. https://doi.org/10.1021/jp802018m.
Miličević, A., Šinko, G., 2021. RETRACTED: Development of a simple QSAR model for reliable evaluation of acetylcholinesterase inhibitor potency. Eur. J. Pharm. Sci. 160, 105757. https://doi.org/10.1016/j.ejps.2021.105757.
Mohammad, D., Chan, P., Bradley, J., Lanctôt, K., Herrmann, N., 2017. Acetylcholinesterase inhibitors for treating dementia symptoms - a safety evaluation. Exp. Opin. Drug Saf. 16 (9), 1009–1019. https://doi.org/10.1080/14740338.2017.1351540.
Niu, B., Zhao, M., Su, Q., Zhang, M., Lv, W., Chen, Q., Chen, F., Chu, D., Du, D., Zhang, Y., 2017. 2D-SAR and 3D-QSAR analyses for acetylcholinesterase inhibitors. Mol. Divers. 21 (2), 413–426. https://doi.org/10.1007/s11030-017-9732-0.
Online SMILES Translator and Structure File Generator, 2020.
Ordentlich, A., Barak, D., Kronman, C., Flashner, Y., Leitner, M., Segall, Y., Ariel, N., Cohen, S., Velan, B., Shafferman, A., 1993. Dissection of the human acetylcholinesterase active center determinants of substrate specificity. Identification of residues constituting the anionic site, the hydrophobic site, and the acyl pocket. J. Biol. Chem. 268 (23), 17083–17095.
Rahman, A., Khalid, A., Sultana, N., Nabeel Ghayur, M., Ahmed Mesaik, M., Riaz Khan, M., Gilani, A.H., Iqbal Choudhary, M., 2006. New natural cholinesterase inhibiting and calcium channel blocking quinoline alkaloids. J. Enzyme Inhib. Med. Chem. 21, 703–710. https://doi.org/10.1080/14756360600889708.
Randić, M., 2008. On history of the Randić index and emerging hostility toward chemical graph theory. MATCH Commun. Math. Comput. Chem. 59, 5–124.
Raos, N., Miličević, A., 2016. How reliable are models based on topological index 3χv for the prediction of stability constants? Croat. Chem. Acta 89 (1), 1–6. https://doi.org/10.5562/cca2723.
Raos, N., Branica, G., Miličević, A., 2008. The use of graph-theoretical models to evaluate two electroanalytical methods for determination of stability constants. Croat. Chem. Acta 81, 511–517 https://hrcak.srce.hr/file/49347.
Rappaport, F., Fischl, J., Pinto, N., 1959. An improved method for the estimation of cholinesterase activity in serum. Clin. Chim. Acta 4 (2), 227–230. https://doi.org/10.1016/0009-8981(59)90134-2.
Reiner, E., Sinko, G., Skrinjarić-Spoljar, M., Simeon-Rudolf, V., 2000. Comparison of protocols for measuring activities of human blood cholinesterases by the Ellman method. Arh. Hig. Rada Toksikol. 51, 13–18 https://hrcak.srce.hr/file/1664.
Rydberg, E.H., Brumshtein, B., Greenblatt, H.M., Wong, D.M., Shaya, D., Williams, L. D., Carlier, P.R., Pang, Y.-P., Silman, I., Sussman, J.L., 2006. Complexes of alkylene-linked tacrine dimers with torpedo c alifornica acetylcholinesterase: binding of Bis(5)-tacrine produces a dramatic rearrangement in the active-site gorge. J. Med. Chem. 49, 5491–5500. https://doi.org/10.1021/jm060164b.
Sanad, S.M.H., Mekky, A.E.M., 2021. Novel nicotinonitrile-coumarin hybrids as potential acetylcholinesterase inhibitors: design, synthesis, in vitro and in silico studies. J. Iran. Chem. Soc. 18 (1), 213–224. https://doi.org/10.1007/s13738-020-02018-6.
Saxena, A., Redman, A.M.G., Jiang, X., Lockridge, O., Doctor, B.P., 1999. Differences in active-site gorge dimensions of cholinesterases revealed by binding of inhibitors to human butyrylcholinesterase. Chem. Biol. Interact. 119–120, 61–69. https://doi.org/10.1016/S0009-2797(99)00014-9.
Selassie, C., Verma, R.P., 2010. History of quantitative structure-activity relationships. In: Burger's Medicinal Chemistry and Drug Discovery. John Wiley & Sons, Inc., Hoboken, NJ, USA. <https://doi.org/10.1002/0471266949.bmc001.pub2>.
Sharma, V., Goswami, R., Madan, A.K., 1997. Eccentric connectivity index: a novel highly discriminating topological descriptor for structure−property and structure−activity studies. J. Chem. Inf. Comput. Sci. 37, 273–282. https://doi.org/10.1021/ci960049h.
Shityakov, S., Broscheit, J., Puskás, I., Roewer, N., Foerster, C., 2014. Three-dimensional quantitative structure-activity relationship and docking studies in a series of anthocyanin derivatives as cytochrome P450 3A4 inhibitors. Adv. Appl. Bioinforma. Chem. 11. https://doi.org/10.2147/AABC.S56478.
Simeon-Rudolf, V., Šinko, G., Štuglin, A., Reiner, E., 2001. Inhibition of human blood acetylcholinesterase and butyrylcholinesterase by ethopropazine. Croat. Chem. Acta 74, 173–182 https://hrcak.srce.hr/file/194637.
Šinko, G., 2019. Assessment of scoring functions and in silico parameters for AChE-ligand interactions as a tool for predicting inhibition potency. Chem. Biol. Interact. 308, 216–223. https://doi.org/10.1016/j.cbi.2019.05.047.
Šinko, G., Čalić, M., Kovarik, Z., 2006. para - and ortho -Pyridinium aldoximes in reaction with acetylthiocholine. FEBS Lett. 580, 3167–3172. https://doi.org/10.1016/j.febslet.2006.04.070.

Šinko, G., Čalić, M., Bosak, A., Kovarik, Z., 2007. Limitation of the Ellman method: Cholinesterase activity measurement in the presence of oximes. Anal. Biochem. 370 (2), 223–227. https://doi.org/10.1016/j.ab.2007.07.023.

Šinko, G., Brglez, J., Kovarik, Z., 2010. Interactions of pyridinium oximes with acetylcholinesterase. Chem. Biol. Interact. 187 (1-3), 172–176. https://doi.org/10.1016/j.cbi.2010.04.017.

Sussman, J.L., Harel, M., Frolow, F., Oefner, C., Goldman, A., Toker, L., Silman, I., 1991. Atomic structure of acetylcholinesterase from Torpedo californica: a prototypic acetylcholine-binding protein. Science (80-). 253 (5022), 872–879.

Tetko, I.V., Gasteiger, J., Todeschini, R., Mauri, A., Livingstone, D., Ertl, P., Palyulin, V. A., Radchenko, E.V., Zefirov, N.S., Makarenko, A.S., Tanchuk, V.Y., Prokopenko, V. V., 2005. Virtual computational chemistry laboratory – design and description. J. Comput. Aided. Mol. Des. 19 (6), 453–463. https://doi.org/10.1007/s10822-005-8694-y.

Wong, K.Y., Mercader, A.G., Saavedra, L.M., Honarparvar, B., Romanelli, G.P., Duchowicz, P.R., 2014. QSAR analysis on tacrine-related acetylcholinesterase inhibitors. J. Biomed. Sci. 21, 84. https://doi.org/10.1186/s12929-014-0084-0.

Xie, J., Liang, R., Wang, Y., Huang, J., Cao, X., Niu, B., 2020. Progress in target drug molecules for Alzheimer's disease. Curr. Top. Med. Chem. 20 (1), 4–36. https://doi.org/10.2174/1568026619666191203113745.

Zandona, A., Katalinić, M., Šinko, G., Radman Kastelic, A., Primožič, I., Kovarik, Z., 2020. Targeting organophosphorus compounds poisoning by novel quinuclidine-3 oximes: development of butyrylcholinesterase-based bioscavengers. Arch. Toxicol. 94 (9), 3157–3171. https://doi.org/10.1007/s00204-020-02811-5.